Swelling of biological and semiflexible polyelectrolytes

2009 J. Phys.: Condens. Matter 21 424112

(http://iopscience.iop.org/0953-8984/21/42/424112)

J. Phys.: Condens. Matter **21** (2009) 424112 (11pp) doi:10.1088/0953-8984/21/42/424112

Swelling of biological and semiflexible polyelectrolytes

Andrey V Dobrynin and Jan-Michael Y Carrillo

Polymer Program, Institute of Materials Science and Department of Physics,
University of Connecticut, Storrs, CT 06269-3136, USA

Received 31 March 2009
Published 29 September 2009
Online at stacks.iop.org/JPhysCM/21/424112

Abstract

We have developed a theoretical model of swelling of semiflexible (biological) polyelectrolytes in salt solutions. Our approach is based on separation of length scales which allowed us to split a chain's electrostatic energy into two parts that describe local and remote electrostatic interactions along the polymer backbone. The local part takes into account interactions between charged monomers that are separated by distances along the polymer backbone shorter than the chain's persistence length. These electrostatic interactions renormalize chain persistence length. The second part includes electrostatic interactions between remote charged pairs along the polymer backbone located at distances larger than the chain persistence length. These interactions are responsible for chain swelling. In the framework of this approach we calculated effective chain persistence length and chain size as a function of the Debye screening length, chain degree of ionization, bare persistence length and chain degree of polymerization. Our crossover expression for the effective chain's persistence length is in good quantitative agreement with the experimental data on DNA. We have been able to fit experimental datasets by using two adjustable parameters: DNA ionization degree ($\alpha = 0.15$–0.17) and a bare persistence length ($l_p = 40$–44 nm).

(Some figures in this article are in colour only in the electronic version)

1. Introduction

Swelling of a polyelectrolyte chain in salt solutions is one of the classical problems of polymer physics [1–3]. The solution of this problem is of paramount importance for understanding the conformational and elastic properties of DNA [4–17]. The first attempt to account for the effect of the electrostatic interactions on conformations of a polyelectrolyte chain was done over 60 years ago by Kuhn, Kunzle and Katchalsky [18, 19] and by Hermans and Overbeek [20]. Balancing a chain conformational entropy with an electrostatic second virial coefficient they established that a polyelectrolyte chain in a salt solution swells with deceasing salt concentration such that a chain size scales with the Debye screening length, κ^{-1}, and the chain degree of polymerization, N, as $R \propto \kappa^{-2/5}N^{3/5}$. This result was unchallenged until 1977 when Odijk [21] and, independently, Skolnick and Fixman [22] established that electrostatic interactions between charged monomers can lead to an additional stiffening of a semiflexible polyelectrolyte chain. They showed that an electrostatic correction to the chain's persistence length l_p^{OSF} is a quadratic function of the Debye screening length, $l_p^{OSF} \sim \kappa^{-2}$. According to this finding a polyelectrolyte chain in a salt solution behaves as a semiflexible polymer whose stiffness could be adjusted by changing salt concentration. Thus, in addition to chain swelling, electrostatic interactions can also change the local chain's bending properties. The combined effect of the electrostatic interactions on the local chain stiffening and swelling was taken into account by Odijk and Houwaart [23]. Their analysis leads to a chain size, $R \propto \kappa^{-3/5}N^{3/5}$, which has a stronger salt concentration dependence than the KKKHO result. Note that the original KKKHO result [18–20] can be derived by assuming a linear scaling of a chain's persistence length with κ^{-1}. Thus, the discrepancy between the two results is due to a different dependence of the chain's persistence length on the Debye radius.

Since the early 1980s development of a theory of a polyelectrolyte chain in salt solutions followed two parallel paths reproducing either a linear [24–33] or quadratic [2, 34–43] dependence of the chain's persistence length on the Debye screening length. Computer simulation results were also more or less equally divided between the two

camps [44–48]. There exists a substantial amount of literature on this subject and it is impossible to cover all of it in a short introduction. A more detailed review of the subject can be found in [1, 3]. Here we will briefly outline only some of the papers to illustrate the different points of view.

The original KKKHO approach [18–20] was improved by Muthukumar [25, 26] who applied the Edwards–Singh variational principle [49] to account for the effect of the electrostatic interactions on a chain's statistics and derived a general expression for a chain size dependence on salt concentration which covered both low and high salt concentration regimes. In the swollen chain regime $R \propto N^{3/5}\kappa^{-2/5}$ scaling is recovered. Schmidt [24] modified a Flory approach to calculate the chain size and persistence length. In this approach the electrostatic energy of the chain was evaluated using the worm-like chain distribution function for the average mean-square distance between monomers. The numerical minimization of the chain's free energy leads to a weaker than κ^{-2} dependence of a chain's persistence length without a pure scaling regime. At high salt concentrations the electrostatic persistence length seems to be approaching κ^{-1} dependence. Barrat and Joanny [27] used a Gaussian variational approach with a trial function describing a chain under tension to describe a chain's bending rigidity. This resulted in a κ^{-1} dependence for the electrostatic persistence length. In a series of papers Ha and Thirumalai [29, 34] applied the Edwards and Singh variational principle [49] minimizing the error in the chain mean-square end-to-end distance between a trial chain and an actual polymer chain. For weakly charged chains the electrostatic persistence length is proportional to κ^{-2}. However, the electrostatic interactions of intermediate strength lead to a linear dependence of the electrostatic persistence length on κ^{-1}. Netz and Orland [39] and Manghi and Netz [40] have applied a Gaussian variational principle with electrostatic persistence length as an adjustable parameter. This approach leads to κ^{-2} dependence of the electrostatic persistence length reproducing Khokhlov–Khachaturian's result for weakly charged chains [50]. However, for a swollen chain regime these calculations led to a surprising size scaling with $R \propto N^{2/3}\kappa^{-2/3}$. An extension of the Muthukumar approach [25, 26] to semiflexible polyelectrolytes was recently done by Ghosh *et al* [51].

Thus, as one can see from our brief overview of the subject the results for the chain size and persistence length scaling depend on approximations used during derivation and particular on how electrostatic interactions at different length scales were taken into account. In this paper we re-examine a problem of swelling of a semiflexible polyelectrolyte chain. We utilize a scale separation approximation in which the effect of the electrostatic interactions can be divided into two parts. The first one represents interactions between the charged pairs located at distances along the polymer backbone shorter than the chain persistence length. These interactions are responsible for the local chain stiffening. The second part of the electrostatic interactions includes interactions between charged groups remote along the polymer backbone and is responsible for the chain swelling effect. We will show how this separation can be done in a consistent manner by using a high temperature expansion when electrostatic interactions can be considered as a weak perturbation and by applying the Edwards–Singh variational principle in a case of electrostatic interactions with arbitrary strength.

The rest of this paper is organized as follows. In section 2 we provide a brief overview of the results for semiflexible chains using a normal mode representation. Section 3 presents calculations of the chain swelling in the framework of a high temperature expansion and Edwards–Singh variational approach. We will also derive a crossover expression for the effective chain's persistence length which accounts for swelling effects. In section 4 we compare our predictions with experimental data for DNA persistence length dependence on a solution ionic strength. Finally, in section 5 we summarize our results.

2. Ideal semiflexible chain

Before addressing the swelling of a semiflexible polyelectrolyte chain we present a brief overview of the general results for an ideal semiflexible chain. Consider a semiflexible chain with the number of bonds N. A chain conformation is described by a set of 3D bond vectors $\{\vec{r}_i\}$, connecting neighboring monomers along the polymer backbone. The potential energy of an ideal semiflexible chain with the reduced bending energy K in a given conformation is

$$\frac{U_0(\{\vec{r}_i\})}{k_B T} = \frac{K}{2}\sum_{i=0}^{N-2}\left(\vec{r}_i - \vec{r}_{i+1}\right)^2 + \frac{\mu_0}{2}\sum_{i=0}^{N-1}\vec{r}_i^{\,2}, \qquad (1)$$

where the second term accounts for the constraint that the bond length is equal to b, k_B is the Boltzmann constant and T is the absolute temperature. The partition function of a semiflexible chain is

$$Z = \int \mathrm{d}\{\vec{r}_i\}\exp\left(-\frac{U_0(\{\vec{r}_i\})}{k_B T}\right) \qquad (2)$$

where integration in equation (2) is performed over the bond vectors $\vec{r}_i$. To calculate the chain partition function and any chain average property it is useful to introduce the set of normal coordinates [49]:

$$\vec{r}_s = \vec{a}_0 + 2\sum_{k=1}^{N-1}\vec{a}_k\cos\left(\frac{\pi k s}{N}\right). \qquad (3)$$

In this representation the chain's potential energy is a quadratic function of the mode amplitudes:

$$\frac{U_0(\{\vec{a}_k\})}{k_B T} = N\sum_{k=1}^{N-1}\left(K\left(\frac{k\pi}{N}\right)^2 + \mu_0\right)\vec{a}_k^{\,2} + \frac{N\mu_0}{2}\vec{a}_0^{\,2} \qquad (4)$$

where we used the approximation $(2(1-\cos q) \approx q^2)$. In the normal mode representation, the bond–bond correlation function $G(n)$, describing the decay of the orientational memory along the polymer backbone,

$$G(n) = \frac{1}{N-n}\sum_{s=0}^{N-n-1}\langle(\vec{r}_s\cdot\vec{r}_{s+n})\rangle_0, \qquad (5)$$

is equal to

$$G(n) = \langle \vec{a}_0^2 \rangle_0 + 2\sum_{k=1}^{N-1} \langle \vec{a}_k^2 \rangle_0 \cos\left(\frac{k\pi n}{N}\right) \tag{6}$$

where brackets $\langle \cdots \rangle_0$ denote averaging with the statistical weight $\exp(-U_0(\{\vec{a}_k\})/k_BT)$. The value of the bond–bond correlation function $G(0)$ should be equal to the square of the bond length, b^2, which imposes a constraint on the mode spectrum:

$$b^2 = \langle \vec{a}_0^2 \rangle_0 + 2\sum_{k=1}^{N-1} \langle \vec{a}_k^2 \rangle_0. \tag{7}$$

We can use this equation as a self-consistency condition determining the relation between the parameters of the chain and the parameter μ_0 in equation (1).

Since the chain's potential energy is a quadratic function of the mode amplitudes, the averaging over the mode amplitudes reduces to calculation of the Gaussian integrals. For a long chain we can substitute summation over the mode number by integration over the wavenumber $q = k\pi/N$ and extend integration to infinity. In this approximation the bond–bond correlation function is equal to

$$G(n) = \frac{3}{\pi}\int_0^\infty \frac{\cos(qn)\,\mathrm{d}q}{Kq^2+\mu_0} = \frac{3}{2\sqrt{\mu_0 K}}\exp\left(-\sqrt{\frac{\mu_0}{K}}n\right). \tag{8}$$

Comparing equation (8) with the bond–bond correlation function of a semiflexible chain with a persistence length l_p and a bond length b, $G(n) = b^2\exp(-bn/l_p)$, we obtain the following relationships between parameters of the chain's potential energy and the chain's bond and persistence lengths:

$$\mu_0 = \frac{3}{2l_p b}, \qquad K = \frac{3l_p}{2b^3}. \tag{9}$$

We will use these relations in section 3 for calculations of the effect of electrostatic interactions on the swelling of a semiflexible polyelectrolyte chain.

3. Swelling of a polyelectrolyte chain

Let us now consider a semiflexible polyelectrolyte chain with fraction of charge monomers α. Here, for simplicity we will assume that a charge is uniformly distributed over all monomers such that each monomer is carrying a fractional charge αe. The potential energy of a polyelectrolyte chain is given by the following expression:

$$\frac{U_{PE}(\{\vec{r}_i\})}{k_BT} = \frac{K}{2}\sum_{i=0}^{N-2}(\vec{r}_i - \vec{r}_{i+1})^2 + \frac{\mu}{2}\sum_{i=0}^{N-1}\vec{r}_i^2 + \frac{l_B\alpha^2}{2}\sum_{i\neq j}^{N}\frac{\exp(-\kappa r_{ij})}{r_{ij}}, \tag{10}$$

where r_{ij} is the distance between monomers i and j on the polymer backbone and $l_B = e^2/\varepsilon k_BT$ is the Bjerrum length (the length scale at which the electrostatic interaction between two elementary charges e in a medium with the dielectric constant ε is equal to the thermal energy k_BT). The Debye screening length κ^{-1} depends on the parameters of the system as $\kappa^2 = 8\pi l_B c_s$, where c_s is the salt concentration. We will separate the electrostatic interactions into two parts. The first one, U_{elec}^{loc}, will account for the electrostatic interactions between pairs of monomers separated by the number of bonds $l < l_{cut}$ and the second one, U_{elec}^{rem}, will take into account electrostatic interactions between remote pairs along the polymer backbone with $l > l_{cut}$. We will also assume that $(\kappa b)^{-1} < l_{cut} \propto l_p/b$. Because of the internal chain bending rigidity the radius vector between monomers i and j along the polymer backbone with distance between them $|i-j| \leqslant l_{cut}$ does not deviate much from a straight line. This permits us to expand the distance between two monomers as follows:

$$r_{ij} = \sqrt{\left(\sum_{s=i}^{j-1}\vec{r}_s\right)^2} \approx bl_{ij}\left(1 + \frac{1}{2l_{ij}b^2}\sum_{s=i}^{j-1}(\vec{r}_s^2 - b^2) - \left(\frac{1}{4l_{ij}^2b^2}\sum_{s,s'=i}^{j-1}(\vec{r}_s - \vec{r}_{s'})^2\right)\right) \tag{11}$$

where $l_{ij} = |j-i|$ is the number of bonds between the ith and jth monomers along the polymer backbone. Using equation (11) we can expand the local electrostatic energy about a rod-like conformation and obtain the following correction to the electrostatic energy of a rod:

$$\frac{\Delta U_{elec}^{loc}(\{\vec{r}_i\})}{k_BT} \approx \frac{u\alpha^2}{b^2}\left(\sum_{\substack{i<j,\\ l_{ij}\leqslant l_{cut}}} V(l_{ij})\left(\frac{l_{ij}}{2}\sum_{s=i}^{j-1}(b^2 - \vec{r}_s^2) + \tfrac{1}{4}\sum_{s,s'=i}^{j-1}(\vec{r}_s - \vec{r}_{s'})^2\right)\right) \tag{12}$$

where u is the ratio of the Bjerrum length l_B to the bond size b, and we introduced a function

$$V(l_{ij}) = \frac{\exp(-\kappa b l_{ij})}{l_{ij}^3}(1 + \kappa b l_{ij}). \tag{13}$$

In the normal mode representation the correction term given by equation (12) is a quadratic function of the mode amplitudes:

$$\frac{\Delta U_{elec}^{loc}(\{\vec{a}_k\})}{k_BT} = \frac{1}{2}Nb^2V_1 - NV_1\frac{\vec{a}_0^2}{2} + N\sum_{k=1}^{N-1}\left(-V_1 + V_2\left(\frac{k\pi}{N}\right)\right)\vec{a}_k^2 \tag{14}$$

where we defined

$$V_1 = \frac{u\alpha^2}{b^2}\sum_{m=1}^{l_{cut}}\left(1 - \frac{m}{N}\right)m^2V(m) \approx -\frac{u\alpha^2}{b^2}\ln(\kappa b) \tag{15a}$$

$$V_2(q) = \frac{2u\alpha^2}{b^2}\sum_{m=1}^{l_{cut}}\left(1 - \frac{m}{N}\right)V(m) \times \left(\sum_{s=1}^{m}(m-s)(1-\cos(qs))\right) \underset{q\ll 1}{\approx} \frac{u\alpha^2}{4\kappa^2b^4}q^2. \tag{15b}$$

Substituting terms describing local electrostatic interactions (see equation (14)) into the expression for the chain's potential

energy equation (10) we obtain

$$\frac{U_{\rm PE}(\{\vec{a}_k\},\hat{\mu})}{k_{\rm B}T} \approx N\sum_{k=1}^{N-1}\left(K\left(\frac{k\pi}{N}\right)^2 + V_2\left(\frac{k\pi}{N}\right) + \hat{\mu}\right)\vec{a}_k^2 + \frac{N\hat{\mu}\vec{a}_0^2}{2} + \frac{l_{\rm B}\alpha^2}{2}\sum_{|j-i|>l_{\rm cut}}^{N}\frac{\exp(-\kappa r_{ij}(\{\vec{a}_k\}))}{r_{ij}(\{\vec{a}_k\})} \tag{16}$$

where we defined $\hat{\mu} = \mu - V_1$ and omitted terms that do not depend on the mode amplitudes.

We will first consider electrostatic interactions between remote pairs along the polymer backbone as a weak perturbation and analyze the effect of the local electrostatic interactions on the renormalization of the chain bending rigidity. Taking this into account we can write the self-consistency relation equation (7) as follows:

$$b^2 = \frac{3}{\pi}\int_0^\infty \frac{{\rm d}q}{Kq^2 + V_2(q) + \hat{\mu}} \approx \frac{3}{\pi}\int_0^\infty \frac{{\rm d}q}{Kq^2 + \frac{u\alpha^2}{4b^4\kappa^2}q^2 + \hat{\mu}} = \frac{3}{2}\frac{1}{\sqrt{\hat{\mu}\left(K + \frac{u\alpha^2}{4b^4\kappa^2}\right)}}. \tag{17}$$

In simplifying equation (17) we utilized a small q expansion of function $V_2(q)$ (see equation (15*b*)). It follows from equation (17) that the effect of the local electrostatic interactions is reduced to renormalization of the chain's bending rigidity. This correction has a well-known OSF form and scales quadratically with the Debye radius κ^{-1}. Solving equation (17) for the parameter $\hat{\mu}$ one obtains

$$\hat{\mu} = \frac{9}{4b^4}\left(K + \frac{u\alpha^2}{4b^4\kappa^2}\right)^{-1} = \frac{9}{4b^4K_{\rm eff}}, \qquad \text{and} \qquad \hat{l}_{\rm p} = l_{\rm p} + \frac{l_{\rm B}\alpha^2}{6\kappa^2b^2}. \tag{18}$$

It is interesting to point out that the numerical coefficient in front of the electrostatic correction to the chain's persistence length (see equations (18)) is different from the one derived by the OSF [21, 22] (it is equal to 1/6 instead of 1/4). The reason for this is a different chain model used to describe a chain bending rigidity (equation (1)). In our model the bending energy term depends on the mutual orientation of the 3D bond vectors $\{\vec{r}_i\}$ instead of 2D unit bond vectors $\{\vec{n}_i\}$ as it is in the original OSF model [21, 22]. Thus, a numerical coefficient is model-dependent and could be written in a general form $1/2D$, where D is the bond vector dimensionality.

In the case of the weak electrostatic interactions their effect on the chain swelling can be evaluated by using a high temperature expansion [49]. In this approximation the mean-square average value of the end-to-end vector $\vec{R}_N$ is

$$\langle R^2\rangle = \langle \vec{R}_N^2(\{\vec{a}_k\})\left(1 - \frac{U_{\rm elec}^{\rm rem}(\{\vec{a}_k\})}{k_{\rm B}T}\right)\right\rangle_w \times \left\langle\left(1 - \frac{U_{\rm elec}^{\rm rem}(\{\vec{a}_k\})}{k_{\rm B}T}\right)\right\rangle_w^{-1} \tag{19}$$

where brackets $\langle\cdots\rangle_w$ denote averaging with the statistical weight

$$w(\{\vec{a}_k\}) = \exp\left(-N\sum_{k=1}^{N-1}\left(K_{\rm eff}\left(\frac{k\pi}{N}\right)^2 + \hat{\mu}\right)\vec{a}_k^2 - \frac{N\hat{\mu}}{2}\vec{a}_0^2\right). \tag{20}$$

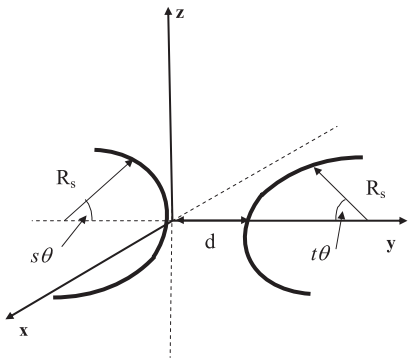

Figure 1. Schematic sketch of two chain sections for calculation of the effective second virial coefficient.

The details of calculations of averages in equation (20) are given in appendix A, below we present a final result:

$$\langle R^2\rangle \approx 2b\hat{l}_{\rm p}N + 4\sqrt{\frac{3}{\pi}}\frac{l_{\rm B}\alpha^2}{\kappa^2\sqrt{\hat{l}_{\rm p}b}}N^{3/2}. \tag{21}$$

Thus, the total effect of the electrostatic interactions is reduced to local chain stiffening which is manifested in renormalization of the chain's persistence length $\hat{l}_{\rm p}$ and additional chain swelling which is due to interactions between remote charges along the polymer backbone. Note that the correction to the ideal chain size (the second term in the rhs of equation (21)) can be interpreted as a result of interactions between monomers with the effective second virial coefficient, $B_{\rm el} \approx 4\pi l_{\rm B}\alpha^2\kappa^{-2}$. This means that interactions between charges are treated as uncorrelated. This approximation fails with increasing value of the Debye screening length when more and more monomers start contributing to the electrostatic repulsion as two chain sections come in contact with each other.

In order to demonstrate the importance of the connectivity effect for calculations of electrostatic interactions between monomers, let us calculate a probability to find two monomers separated by s bonds ($s \gg \hat{l}_{\rm p}/b$) along the polymer backbone at a distance d and oriented with respect to each other with an angle γ (see figure 1):

$$P(d,\gamma) \propto \exp\left(-\frac{U_{\rm int}(d,\gamma,\theta)}{k_{\rm B}T}\right)\exp\left(-\frac{3d^2}{4b\hat{l}_{\rm p}s}\right) \tag{22}$$

where $U_{\rm int}(d,\gamma,\theta)$ is the energy of two chain segments containing test monomers. This energy includes bending and electrostatic energy contributions. In order to obtain an explicit form of the interaction energy $U_{\rm int}(d,\gamma,\theta)$, we will assume that both chain's sections have circular conformations with a radius of curvature R_s and with an angle θ between two neighboring bond vectors along the polymer backbone (see figure 1), $R_s\theta \approx b$. The bending energy of two chain sections in a circular conformation with $n_p \approx \pi/\theta$ bonds is estimated as

$$\frac{U_{\rm bend}(\theta)}{k_{\rm B}T} \approx 2n_p\frac{K_{\rm eff}b^2\theta^2}{2} \approx \pi K_{\rm eff}b^2\theta. \tag{23}$$

Note that one can consider a circular conformation as a directed walk in which a chain makes a turn by π radians after n_p steps.

The energy of electrostatic interactions between two sections in a circular conformation is equal to (see appendix B for details)

$$\frac{U_{\rm el}(d,\gamma,\theta)}{k_{\rm B}T} \approx \frac{2\pi l_{\rm B}\alpha^2 \exp(-d\kappa)}{\kappa b\sqrt{b^2\sin^2\gamma + d\theta(2b+d\theta)}}. \quad (24)$$

In the limit of $\theta = 0$ equation (24) is reduced to the electrostatic energy of two interacting rods. The optimal value of the bending angle θ as a function of the segment separation and mutual orientation is obtained by optimizing both bending and electrostatic energies with respect to an angle θ. By performing differentiations of equation (23) and (24) one has

$$\left(\frac{u\alpha^2 d}{\kappa b K_{\rm eff} b^3}\right)^{2/3} \approx \left(\frac{u\alpha^2 d}{\kappa b \hat{l}_{\rm p}}\right)^{2/3} \approx \sin^2\gamma + 2d\theta/b. \quad (25)$$

In simplifying equation (25) we have assumed that $d\theta/b \ll 1$, $K_{\rm eff}b^3 \propto \hat{l}_{\rm p}$ and omitted numerical coefficients. Analysis of equation (24) shows that the maximum segment deformation occurs when both chain sections align in the same plane, $\gamma = 0$. For this orientation the bending angle is of the order of

$$\theta \approx \left(\frac{u\alpha^2 b^{1/2}}{\kappa \hat{l}_{\rm p} d^{1/2}}\right)^{2/3}. \quad (26)$$

By substituting this value of the chain bending angle into equation (24) one can show that the local chain bending will influence the probability function equation (22) only for the range of orientation angles $\gamma \leqslant (\frac{u\alpha^2 d}{\kappa \hat{l}_{\rm p} b})^{1/3}$. This interval is narrow if the parameter $\frac{u\alpha^2 d}{\kappa \hat{l}_{\rm p} b} \approx \frac{u\alpha^2}{\kappa^2 b \hat{l}_{\rm p}} d\kappa \ll 1$. Note that it is true in both cases of weak ($\hat{l}_{\rm p} \propto l_{\rm p}$) and strong ($\hat{l}_{\rm p} \approx u\alpha^2/\kappa^2 b \gg l_{\rm p}$) renormalization of the chain persistence length by the local electrostatic interactions. (Here we are interested in the interval $\kappa d \leqslant 1$, because for larger separations $d > \kappa^{-1}$ the electrostatic interactions decay exponentially.) Thus, for the orientation angles $\gamma \geqslant (\frac{u\alpha^2 d}{\kappa \hat{l}_{\rm p} b})^{1/3}$ the total interaction energy can be approximated by its electrostatic part [52]

$$\frac{U_{\rm int}(d,\gamma,0)}{k_{\rm B}T} \approx \frac{2\pi l_{\rm B}\alpha^2 \exp(-d\kappa)}{\kappa b^2 |\sin\gamma|}. \quad (27)$$

Analyzing the probability function, equation (22), with the interaction energy given by equation (27) one can conclude that the electrostatic interactions between chain sections will create a correlation hole with a size of the order of κ^{-1} around a chain when $u\alpha^2 > \kappa b$. In this range of parameters evaluation of the electrostatic interactions between chain sections requires taking into account the effect of charge connectivity. This effect can be accounted for approximating electrostatic interactions by an effective second virial coefficient.

We can use the interaction energy given by equation (27) to evaluate an effective second virial coefficient between charged monomers as

$$B_{\rm el} \approx 2b^2 \int_0^{\pi/2} \sin^2\gamma\, {\rm d}\gamma \times \int_b^\infty \left(1 - \exp\left(-\frac{U_{\rm int}(r,\gamma,0)}{k_{\rm B}T}\right)\right) {\rm d}r. \quad (28)$$

Fixman and Skolnick [52] showed that equation (28) has two simple asymptotic regimes:

$$B_{\rm el} \approx \begin{cases} 4\pi l_{\rm B}\alpha^2\kappa^{-2}, & \text{for } u\alpha^2 \ll \kappa b \\ \frac{\pi}{4} b^2 \kappa^{-1} \ln(l_{\rm B}\alpha^2/\kappa b^2), & \text{for } \kappa b \ll u\alpha^2. \end{cases} \quad (29)$$

Using equations (29) for the monomer excluded volume we can rewrite equation (21) as follows:

$$\langle R^2\rangle \approx 2b\hat{l}_{\rm p}N + \sqrt{\frac{3}{\pi^3}}\frac{N^{3/2}}{\sqrt{\hat{l}_{\rm p}b}} \times \begin{cases} 4\pi l_{\rm B}\alpha^2\kappa^{-2}, & \text{for } u\alpha^2 \ll \kappa b \\ \pi b^2\kappa \ln(l_{\rm B}\alpha^2/\kappa b^2), & \text{for } \kappa b \ll u\alpha^2. \end{cases} \quad (30)$$

The high temperature expansion breaks down when the value of the Fixman parameter $B_{\rm el}N^{1/2}/(\hat{l}_{\rm p}b)^{3/2}$ becomes of the order of unity.

In order to obtain a chain size for arbitrary salt concentration range we will use the Edwards–Singh variational principle [49]. In the framework of this approach the chain size is given by a solution of the following equation (see appendix C for details):

$$\frac{l_{\rm p}^{\rm tr}}{\hat{l}_{\rm p}} - 1 - \frac{3^{1/2}}{2\pi^{3/2}}\frac{B_{\rm el}N^{1/2}}{(l_{\rm p}^{\rm tr}b)^{3/2}}\left(1 - \frac{3}{2}\sqrt{\frac{\hat{l}_{\rm p}}{bN}} + \frac{1}{2}\left(\frac{\hat{l}_{\rm p}}{bN}\right)^{3/2}\right) = 0. \quad (31)$$

Equation (31) can be considered as a self-consistent equation for the effective chain's persistence length $l_{\rm p}^{\rm tr}$. Note that, by using relationships between a chain persistence length and chain size $\langle R^2\rangle = 2bl_{\rm p}^{\rm tr}N$ and $R_0^2 = 2b\hat{l}_{\rm p}N$, one can rewrite equation (31) in a form similar to the Flory-like expression for an equilibrium chain size [49]. It is important to point out that for the case of weak electrostatic interactions their contribution to the effective monomeric second virial coefficient has to be supplemented by the second virial coefficient due to excluded-volume (hard-core) interactions, $B_0 \approx \pi b^3/2$, in obtaining which we have performed angle averaging of the excluded volume of two rods. This modification allows us to capture a crossover to a neutral chain regime. Solving equation (31) for a chain persistence length and using a relation between the chain's persistence length and a chain size, $\langle R^2\rangle \propto bl_{\rm p}^{\rm tr}N$, one has

$$\langle R^2\rangle^{1/2} \propto N^{3/5}(l_{\rm p}b^4)^{1/5} \begin{cases} (1 + u\alpha^2(\kappa b)^{-2})^{1/5}, \\ \quad \text{for } u\alpha^2 \ll \kappa b \\ (\kappa b)^{-1/5}, \\ \quad \text{for } (u\alpha^2 b/l_{\rm p})^{1/2} \ll \kappa b \ll u\alpha^2. \end{cases} \quad (32)$$

To complete our analysis of swelling of a semiflexible polyelectrolyte chain we have to consider the interval of salt concentrations for which $\kappa b \ll (u\alpha^2 b/l_{\rm p})^{1/2}$. In this salt concentration range the local electrostatic interactions provide a major contribution to the chain's persistence length, $\hat{l}_{\rm p} \approx u\alpha^2/\kappa^2 b$ (see equations (18)). Taking this into account we obtain

$$\langle R^2\rangle^{1/2} \propto N^{3/5} b (u\alpha^2)^{1/5} (\kappa b)^{-3/5}, \quad \text{for } \kappa b \ll (u\alpha^2 b/l_{\rm p})^{1/2}. \quad (33)$$

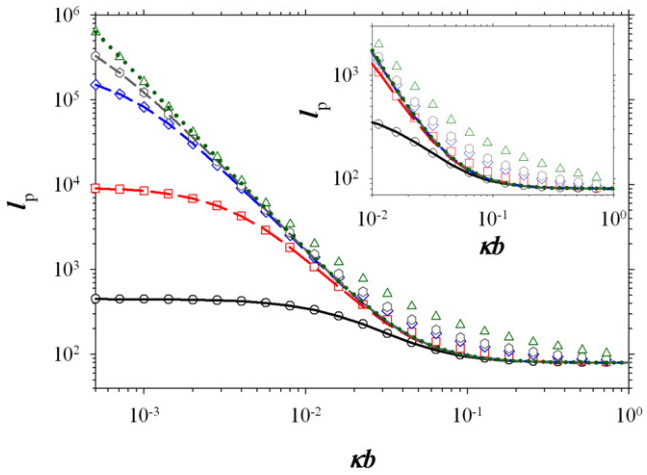

Figure 2. Dependence of the chain's persistence lengths l_p^{tr} (symbols) and $\hat{l}_p$ (lines) on the Debye screening length for semiflexible polyelectrolyte chains with $l_B = b$, $\alpha = 1$ and $l_p = 80b$ for different chain degrees of polymerization: $N = 200$ (circles and black line); $N = 10^3$ (squares and red line); $N = 5 \times 10^3$ (rhomboidss and blue line); $N = 10^4$ (hexagons and gray line); $N = 10^6$ (triangles and dotted line).

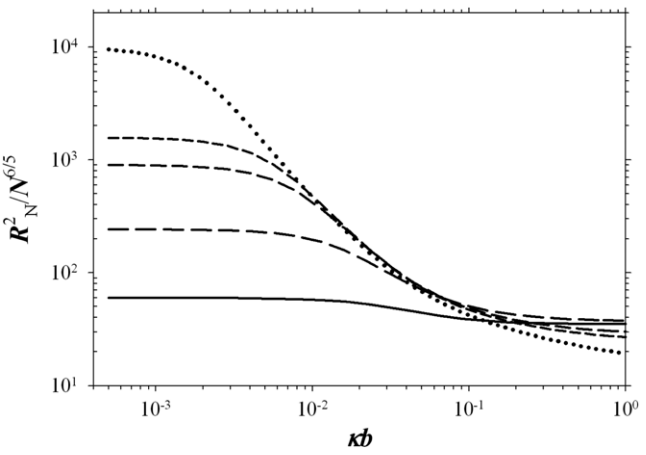

Figure 3. Dependence of the normalized chain size $R_N^2/N^{6/5}$ on the Debye screening length for semiflexible polyelectrolyte chains with $l_B = b$, $\alpha = 1$, $l_p = 80b$ and different chain degrees of polymerizations: $N = 200$ (solid line); $N = 10^3$ (dashed line); $N = 5 \times 10^3$ (dashed–dotted line); $N = 10^4$ (short-dashed line); $N = 10^6$ (dotted line).

Our scaling exponents for the chain size dependence on the Debye screening length are different from the ones obtained by Ghosh *et al* [51]. The origin of this discrepancy is due to the different consideration of the electrostatic interactions. In the Ghosh *et al* approach [51] the electrostatic interactions between charges are always treated as uncorrelated, effectively substituting these interactions by an effective second virial coefficient, $B_{el} \propto \kappa^{-2}$. In our approach we used two different forms for the electrostatic second virial coefficient. In the case of weak electrostatic interactions the connectivity of the charges into the polymer backbone can be neglected resulting in the expression for the electrostatic second virial coefficient to be similar to the ones used by Ghosh *et al* [51], $B_{el} \propto \kappa^{-2}$. However, in the case of the strong electrostatic interactions, when the electrostatic repulsion, $U \propto k_B T(l_B g^2 \kappa)$ between g charges within the Debye screening length, $g \propto \alpha/\kappa b$, is much larger than the thermal energy $U \gg k_B T$, $u\alpha^2 > \kappa b$, the connectivity of the charged monomers into a chain plays an important role. This is manifested in the appearance of the correlation hole with size of the order of the Debye screening length surrounding the polymer backbone. Another origin for the discrepancy between the results is explicit consideration of the renormalization of the chain's persistence length by the local electrostatic interactions adopted in our paper. This was not done in the Ghosh *et al* paper [51].

In figure 2 we show the results of numerical optimization of equation (31) with the value of the second virial coefficient represented by a sum, $B_0 + B_{el}$, where the electrostatic part of the second virial coefficient is given by equation (B.12) for polyelectrolyte chains with different degrees of polymerizations and the bare persistence length $l_p = 80b$. We have also used a more general expression for the chain's persistence length:

$$\hat{l}_p \approx l_p + \frac{l_B \alpha^2}{18} \sum_{m=1}^{N} \left(1 - \frac{m}{N}\right) \exp(-\kappa b m)(1 + \kappa b m) m \quad (34)$$

which accounts for a finite chain size effect (see equation (15*b*)). In equation (34) we have extended summation up to N because $\hat{l}_p \gg \kappa^{-1}$. As one can see from this figure the values of the chain's persistence lengths l_p^{tr} and $\hat{l}_p$ converge with increasing the Debye screening length. This is due to the fact that the value of the effective Fixman parameter (the last term in the lhs of equation (31)) describing the strength of the interactions between remote charged pairs along the polymer backbone decreases with decreasing number of persistent segments per chain $Nb/\hat{l}_p$. The largest difference between the two persistence lengths is observed at intermediate salt concentrations when the value of the electrostatic excluded volume is large enough and at the same time there is a sufficient number of chain persistent segments to elevate a chain swelling. The value of the persistence length saturates when the Debye screening length becomes of the order of the chain's contour length, $\kappa b N \approx 1$. In figure 3 we have used results for l_p^{tr} and plotted the dependence of a normalized value of the chain size $R_N^2/N^{6/5}$ on the Debye screening length. In obtaining the chain size we used equation (A.9) with the persistence length being equal to l_p^{tr}. One can clearly see the existence of the universal regime at the intermediate values of the Debye screening length where the lines corresponding to swelling of chains with different degrees of polymerization coincide. However, the width of this universal regime is relatively narrow. This indicates that it would be challenging to observe pure scaling regimes either in computer simulations or experimentally.

4. Comparison with experiments

DNA is the most studied example of semiflexible polyelectrolytes [4–17]. The effect of salt concentration on

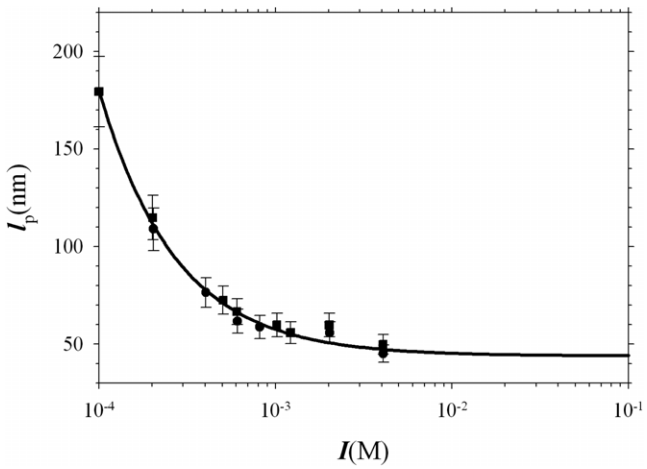

Figure 4. Dependence of the DNA persistence length on the solution ionic strength I obtained by Hagerman for short fragments of DNA (587 and 434 bp) [5]. The solid line is the best fit given by equation (36).

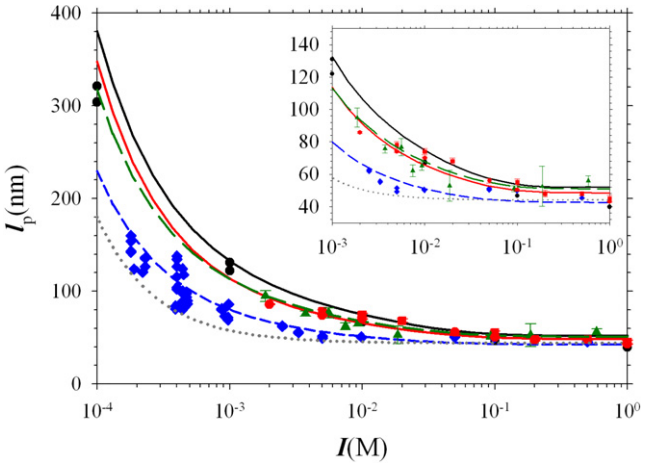

Figure 5. Dependence of the DNA persistence length on the solution ionic strength I. Blue rhomboids show data by Maret and Weill on the lyophilized erythrocyte DNA ($M_w = 4.2 \times 10^6$ g mol^{-1}) [6]. The blue short-dashed line is the best fit to equation (37) with ionization degree $\alpha = 0.15$, bare persistence length $l_p = 40$ nm and degree of polymerization $N = 1.27 \times 10^4$. Green triangles show data by Baumann *et al* on λ-DNA ($M_w = 3.2 \times 10^7$ g mol^{-1}) [15]. The green long-dashed line is the best fit with $\alpha = 0.15$, $l_p = 44$ nm, $N = 9.7 \times 10^4$. Red circles [9] and red squares [7] are data on T7 bacteriophage DNA ($M_w = 2.65 \times 10^7$ g mol^{-1}). The red line is the best fit with $\alpha = 0.17$, $l_p = 42$ nm, $N = 8.03 \times 10^4$. Black circles are data by Makita *et al* on T4 DNA (165.6 kbp) [12]. The black line is the best fit with $\alpha = 0.15$, $l_p = 40$ nm, $N = 3.3 \times 10^5$. The dotted line corresponds to persistence length of a short DNA without swelling effects (see figure 4).

conformational properties of DNA was studied by light scattering [7], by force-extension experiments [15], by transient electric birefringence [5], by magnetic birefringence [6], by flow birefringence [9] and by fluorescence microscopy [12, 14]. The main goal of these research efforts was to find a salt concentration dependence of the DNA persistence length. One has to keep in mind that the obtained value of a chain's persistence length is a function of the method used. For example, in scattering and fluorescence microscopy measurements, the experimentally measured electrostatic persistence length heavily relies on the relation between a chain size and its persistence length:

$$\langle R^2 \rangle \propto b l_p^{\text{eff}} N. \tag{35}$$

Unfortunately, this relation provides an actual value of the chain's persistence length only when there are no additional chain swelling effects. This is usually true for relatively short chains and low salt concentrations when the contribution of the electrostatic interactions between remote charged pairs along the polymer backbone is small. The crossover to the swollen chain regime occurs at salt concentrations where the value of the Fixman interaction parameter becomes of the order of unity. In this case a chain persistence length obtained from equation (35) includes a chain swelling effect and cannot be considered as a local chain property. Thus, in comparing experimental data with the model one has to pay close attention to the method used for extracting a persistence length.

In figure 4 we show experimental data by Hagerman for short fragments of DNA (587 and 434 bp) [5]. The data points can be described by a function

$$l_p^{\text{exp}} \approx 44 \text{ nm} + \frac{0.0136}{I} \tag{36}$$

where I is the solution ionic strength (for the monovalent salts it is equal to the solution salt concentration, $I = c_s$). Using the expression for the chain persistence length equation (18) and assuming that the distance between phosphate groups on the DNA $d_{ph} = 0.34$ nm (there are about 10 base pairs per DNA double helix turn with length 3.4 nm) and the Bjerrum length $l_B = 0.7$ nm we can estimate an effective chain's ionization degree $\alpha \approx 0.19$ corresponding to the best fit given by equation (36). In obtaining the degree of ionization α we have approximated DNA by a rod with a charge density of 20 charges per 3.4 nm, which gives us a distance between effective charges to be equal to $b = 0.17$ nm. For the OSF model [21, 22] the numerical coefficient in front of the electrostatic correction term is 1/4 instead of 1/6. In this case the ionization degree is $\alpha_{\text{OSF}} \approx 0.154$. In our recent paper we have performed molecular dynamics simulations of semiflexible polyelectrolyte chains at different salt concentrations [53]. The best fit to the simulation data corresponds to $\Delta l_p \approx 0.264 \frac{l_B \alpha^2}{(\kappa b)^2}$, which gives a fractional charge per phosphate group to be equal to $\alpha \approx 0.151$.

In figure 5 we have combined results for the effective DNA persistence length obtained by fluorescence microscopy [12], magnetic birefringence [9], force-extension measurements [15] and light scattering [7] and fitting of the experimental data to the effective persistence length given by the following equation:

$$\frac{l_p^{\text{tr}}}{\hat{l}_p} - 1 - \frac{3^{1/2}}{2\pi^{3/2}} \frac{(B_{\text{el}} + B_0) N^{1/2}}{(l_p^{\text{tr}} b)^{3/2}} \times \left(1 - \frac{3}{2}\sqrt{\frac{\hat{l}_p}{bN}} + \frac{1}{2}\left(\frac{\hat{l}_p}{bN}\right)^{3/2}\right) = 0 \tag{37}$$

where the value of the electrostatic second virial coefficient was calculated by numerical integration of equation (B.12)

with a hard-core DNA diameter $d_0 = 2$ nm. The value of the hard-core second virial coefficient B_0 was equal to $B_0 = \pi b^2 d_0/2 \approx \pi(0.17)^2 2.0/2 \approx 9.1 \times 10^{-2}$ nm^3. We have also corrected a value of the numerical coefficient in equation (18) for the chain's persistence length $\hat{l}_p$ to 0.264 in agreement with our simulation results [53]. As one can see all five different datasets can be fitted to equation (37) with close values of the adjustable parameters $\alpha = 0.15$–0.17 and a bare persistence length $l_p = 40$–44 nm. There is a systematic trend showing an increase in the value of the effective chain's persistence length with increasing the chain's degree of polymerization N. This is in agreement with plots shown in figure 2 and is expected for systems where swelling effects play an important role in controlling chain bending properties. It is also important to point out that data points for Bowmann *et al* [15] obtained from DNA stretching experiments can also be fitted to equation (37) with the same value of the ionization degree, $\alpha = 0.15$. Thus, our analysis of Bowmann's data [15] shows that for their DNA samples with the number of base pairs ∼48.5 kbp swelling effects are important. (The number of base pairs was estimated by using for DNA contour length 16.5 μm.) The agreement between theory and experiments is very good since we used only known parameters to describe the structure of DNA and adjusted chain's degree of ionization and the bare persistence length. Note that for our ionization degree the distance between ionized groups $l_{ion} \approx b/\alpha \approx 1$–$1.13$ nm is larger than the value of the Bjerrum length $l_B \approx 0.7$ nm. Thus, there is less than one charge per Bjerrum length.

5. Conclusions

Using high temperature expansion and Edwards–Singh variational principle [49] we have calculated dependence of the size of the semiflexible polyelectrolyte chain on salt concentration. The new feature that sets this study apart from the previous work is the explicit separation of the electrostatic interaction term into local and remote parts. The local part accounts for electrostatic interactions between pairs of charged monomers separated by distances along the polymer backbone smaller or of the order of the chain's persistence length. At these length scales the internal chain bending rigidity preserves a chain conformation close to rod-like. We have exploited this fact and have been able to calculate the effect of the local electrostatic interactions on stiffening of a polyelectrolyte chain. The electrostatic correction to the local chain bending rigidity has a well-known OSF-like form [21, 22] and increases quadratically with the Debye screening length, $\hat{l}_p \propto \kappa^{-2}$. The second part of the chain's electrostatic energy, which accounts for interactions between remote charged pairs along the polymer backbone, is responsible for chain swelling. There are three different scaling regimes in dependence of the chain size on the Debye screening length. At high salt concentrations, the chain size scales with salt concentration as $R \propto c_s^{-1/5}$. At intermediate salt concentrations the strong electrostatic interactions between chain sections create a correlation hole around the chain backbone with a size of the order of the Debye screening length, κ^{-1}. This weakens the salt dependence of the chain size, $R \propto c_s^{-1/10}$. But still the interactions between remote charged pairs along the polymer backbone dominate the chain swelling behavior. Finally, at low salt concentration the local electrostatic interactions begin to dominate the chain's bending rigidity such that the chain's persistence length increases with decreasing salt concentration as $\hat{l}_p \propto c_s^{-1}$. The combination of the local chain stiffening and electrostatic excluded volume results in a stronger dependence of the chain size on salt concentrations, $R \propto c_s^{-3/10}$. Note that in this regime the scaling of the chain size dependence on salt concentration coincides with the one found for flexible polyelectrolytes [47]. It should not be surprising since, at low salt concentrations, the electrostatic interactions play a dominant role completely renormalizing the bare chain's properties.

Our expression for an effective chain persistence length equation (37) is capable of describing all sets of experimental data on DNA by using only two adjustable parameters: DNA ionization degree $\alpha \approx 0.15$–0.17 and a bare persistence length $l_p \approx 40$–44 nm. This is a remarkable achievement which could serve as an experimental verification of our assumption for separation of the length scales. We hope that this work will inspire further studies of semiflexible polyelectrolytes to establish general scaling laws for this type of charged systems.

Acknowledgments

The authors are grateful for support of this research to the Donors of the American Chemical Society Petroleum Research Fund under grant PRF no. 44861-AC7.

Appendix A

In this appendix we present details of the calculations of the chain size using the high temperature expansion. To obtain the chain size we have to calculate the following averages:

$$\begin{aligned}\langle R^2\rangle &\approx \left\langle \vec{R}_N^2(\{\vec{a}_k\})\left(1-\frac{U_{elec}^{rem}(\{\vec{a}_k\})}{k_BT}\right)\right\rangle_w \\ &\quad\times\left\langle\left(1+\frac{U_{elec}^{rem}(\{\vec{a}_k\})}{k_BT}\right)\right\rangle_w \\ &\approx \langle \vec{R}_N^2(\{\vec{a}_k\})\rangle_w + \left\langle\frac{U_{elec}^{rem}(\{\vec{a}_k\})}{k_BT}\right\rangle_w \langle \vec{R}_N^2(\{\vec{a}_k\})\rangle_w \\ &\quad-\left\langle \vec{R}_N^2(\{\vec{a}_k\})\frac{U_{elec}^{rem}(\{\vec{a}_k\})}{k_BT}\right\rangle_w \end{aligned} \tag{A.1}$$

where averaging is performed with the statistical weight given by equation (20). We will first calculate the average value $\langle \vec{R}_N^2(\{\vec{a}_k\})\rangle_w$. In calculating this average it is useful to introduce a generating function

$$Z(q) = \langle \exp(i(\vec{q}\cdot\vec{R}_N))\rangle_w = \left\langle \exp\left(i\left(\vec{q}\cdot\sum_{s=0}^{N-1}\vec{r}_s\right)\right)\right\rangle_w . \tag{A.2}$$

The mean-square average value of the end-to-end distance is obtained by taking a derivative of the generating function with respect to q:

$$\langle \vec{R}_N^2(\{\vec{a}_k\})\rangle_w = -\Delta_{\vec{q}} Z(q)|_{q=0}. \tag{A.3}$$

To calculate averages in the generating function we will use a normal mode representation of the bond vectors:

$$\vec{r}_s = \vec{a}_0 + 2\sum_{k=1}^{N-1} \vec{a}_k \cos\left(\frac{\pi k s}{N}\right). \tag{A.4}$$

Using this representation we can write

$$Z(q) = \left\langle \exp\left(\mathrm{i}\left(\vec{q}\cdot\left(\vec{a}_0 t_0(N) + \sum_{k=1}^{N-1}\vec{a}_k t_k(N)\right)\right)\right)\right\rangle_w \tag{A.5}$$

where we introduced

$$t_k(N) = \sum_{s=0}^{N-1} \cos\left(\frac{\pi k s}{N}\right). \tag{A.6}$$

Since the chain's potential energy is a quadratic function of the mode amplitudes the averaging in equation (A.5) can be explicitly performed resulting in

$$Z(q) = \exp\left(-\frac{q^2 t_0^2(N)}{2N\hat{\mu}} - \frac{q^2}{N}\sum_{k=1}^{N-1}\frac{t_k^2(N)}{(K_{\mathrm{eff}}\hat{k}^2 + \hat{\mu})}\right) \tag{A.7}$$

where $\hat{k} = \pi k/N$. In the limit of large N the summation in equation (A.7) can be transformed to integration:

$$\begin{aligned} Z(q) &\approx \exp\left(-\frac{q^2}{2}\sum_{s,s'=0}^{N-1}\frac{1}{\pi}\int_0^\infty \frac{\cos(x(s-s'))\,\mathrm{d}x}{K_{\mathrm{eff}}x^2 + \hat{\mu}}\right) \\ &= \exp\left(-\frac{q^2}{4}\sum_{s,s'=0}^{N-1}\frac{\exp\left(-\sqrt{\frac{\hat{\mu}}{K_{\mathrm{eff}}}}|s-s'|\right)}{\sqrt{\hat{\mu}K_{\mathrm{eff}}}}\right). \end{aligned} \tag{A.8}$$

The summation over s and s' can be easily performed:

$$R_N^2(\hat{l}_\mathrm{p}) = 2\hat{l}_\mathrm{p}^2(\exp(-bN/\hat{l}_\mathrm{p}) + (bN/\hat{l}_\mathrm{p}) - 1) \approx 2b\hat{l}_\mathrm{p}N. \tag{A.9}$$

In writing the final answer we have assumed that $bN/\hat{l}_\mathrm{p} \gg 1$. Taking this into account we can write down the final expression for the generating function:

$$Z(q) \approx \exp\left(-\frac{q^2 R_N^2(\hat{l}_\mathrm{p})}{6}\right) \approx \exp\left(-\frac{q^2 b\hat{l}_\mathrm{p}N}{3}\right). \tag{A.10}$$

Performing differentiation with respect to q one obtains

$$\langle \vec{R}_N^2(\{\vec{a}_k\})\rangle_w = -\Delta_{\vec{q}} Z(q)|_{q=0} \approx 2b\hat{l}_\mathrm{p}N. \tag{A.11}$$

In performing averaging of the electrostatic interactions $\langle \frac{U_{\mathrm{elec}}^{\mathrm{rem}}(\{\vec{a}_k\})}{k_\mathrm{B}T}\rangle_w$ we need to know the average value of

$$\begin{aligned} \left\langle \frac{l_\mathrm{B}\alpha^2}{r_{nm}}\exp(-r_{mn}\kappa)\right\rangle_w &= l_\mathrm{B}\alpha^2\int\frac{\mathrm{d}^3q}{(2\pi)^3}\frac{4\pi}{q^2+\kappa^2} \\ &\times \langle\exp(\mathrm{i}(\vec{q}\cdot\vec{r}_{mn}))\rangle_w. \end{aligned} \tag{A.12}$$

The averaging of the exponential function is performed similar to the averaging of the generating function equation (A.7) resulting in

$$\begin{aligned} \langle\exp(\mathrm{i}(\vec{q}\cdot\vec{r}_{mn}))\rangle_w &= \left\langle\exp\left(\mathrm{i}\left(\vec{q}\cdot\sum_{s=m}^{n-1}\vec{r}_s\right)\right)\right\rangle_w \\ &= \exp\left(-\frac{q^2 R_{mn}^2}{6}\right) \end{aligned} \tag{A.13}$$

where

$$\begin{aligned} R_{mn}^2(\hat{l}_\mathrm{p}) &= 2\hat{l}_\mathrm{p}^2(\exp(-b|m-n|/\hat{l}_\mathrm{p}) + (b|m-n|/\hat{l}_\mathrm{p}) - 1) \\ &\approx 2b\hat{l}_\mathrm{p}|m-n|. \end{aligned} \tag{A.14}$$

In simplifying the last expression we take into account the fact that the electrostatic energy term only contains pairs of monomers separated by a distance bigger or of the order of the chain persistence length. Performing averages in (A.12) one has

$$\begin{aligned} \left\langle \frac{l_\mathrm{B}\alpha^2}{r_{nm}}\exp(-r_{mn}\kappa)\right\rangle_w &\approx \frac{2l_\mathrm{B}\alpha^2}{\pi}\int_0^\infty \frac{\mathrm{d}q\,q^2}{q^2+\kappa^2} \\ &\times \exp\left(-\frac{q^2 b\hat{l}_\mathrm{p}}{3}|m-n|\right). \end{aligned} \tag{A.15}$$

Now we need the average $\langle \vec{R}_N^2(\{\vec{a}_k\})\frac{U_{\mathrm{elec}}^{\mathrm{rem}}(\{\vec{a}_k\})}{k_\mathrm{B}T}\rangle_w$ to complete calculations for the chain size. This average requires knowledge of the averages in the following form:

$$\begin{aligned} \left\langle \vec{R}_N^2(\{\vec{a}_k\})\frac{l_\mathrm{B}\alpha^2}{r_{nm}}\exp(-r_{mn}\kappa)\right\rangle_w &= -l_\mathrm{B}\alpha^2\int\frac{\mathrm{d}^3q}{(2\pi)^3} \\ &\times \frac{4\pi}{q^2+\kappa^2}\Delta_{q_1}\langle\exp(\mathrm{i}(\vec{q}\cdot\vec{r}_{mn} + \vec{q}_1\cdot\vec{R}_N))\rangle_w|_{q_1=0}. \end{aligned} \tag{A.16}$$

The calculation of the average on the rhs of equation (A.16) is similar to the ones already performed. The answer is

$$\begin{aligned} \langle\exp(\mathrm{i}(\vec{q}\cdot\vec{r}_{mn} + \vec{q}_1\cdot\vec{R}_N))\rangle_w &= \exp\left(-\frac{q^2 R_{mn}^2(\hat{l}_\mathrm{p})}{6}\right. \\ &\left. - \frac{q_1^2 R_N^2(\hat{l}_\mathrm{p})}{6} - 2(\vec{q}_1\cdot\vec{q}_2)I_1(m,n,\hat{l}_\mathrm{p})\right) \end{aligned} \tag{A.17}$$

where we introduced the function

$$\begin{aligned} I_1(m,n,\hat{l}_\mathrm{p}) &= \frac{b^2}{6}\sum_{s=0}^{N-1}\sum_{s'=m}^{n-1}\exp(-|s-s'|b/\hat{l}_\mathrm{p}) \\ &= \tfrac{1}{6}(2b\hat{l}_\mathrm{p}(m-n) - \hat{l}_\mathrm{p}^2(1-\exp(-b(n-m)/\hat{l}_\mathrm{p})) \\ &\times [\exp(-(N-n)b/\hat{l}_\mathrm{p}) + \exp(-mb/\hat{l}_\mathrm{p})]) \\ &\approx \frac{b\hat{l}_\mathrm{p}(m-n)}{3}. \end{aligned} \tag{A.18}$$

In simplifying the last expression we have assumed that the chain is long enough such that one can neglect the end effects (omit terms in the square brackets). In this approximation the average is

$$\begin{aligned} &\left\langle \vec{R}_N^2(\{\vec{a}_k\})\frac{l_\mathrm{B}\alpha^2}{r_{nm}}\exp(-r_{mn}\kappa)\right\rangle_w \\ &= \langle\vec{R}_N^2(\{\vec{a}_k\})\rangle_w\left\langle\frac{l_\mathrm{B}\alpha^2}{r_{nm}}\exp(-r_{mn}\kappa)\right\rangle_w \\ &- \frac{2l_\mathrm{B}\alpha^2}{\pi}\left(\frac{2b\hat{l}_\mathrm{p}(m-n)}{3}\right)^2\int_0^\infty\frac{\mathrm{d}q\,q^4}{q^2+\kappa^2} \\ &\times \exp\left(-\frac{q^2 b\hat{l}_\mathrm{p}|m-n|}{3}\right). \end{aligned} \tag{A.19}$$

Thus, collecting all terms together we finally obtain for the chain size

$$\begin{aligned} \langle\vec{R}_N^2\rangle_w &= 2b\hat{l}_\mathrm{p}N + \frac{2l_\mathrm{B}\alpha^2}{\pi}\sum_{m=l_{\mathrm{cut}}}^{N}(N-m)\left(\frac{2b\hat{l}_\mathrm{p}m}{3}\right)^2 \\ &\times \int_0^\infty\frac{\mathrm{d}q\,q^4}{q^2+\kappa^2}\exp\left(-\frac{q^2 b\hat{l}_\mathrm{p}m}{3}\right). \end{aligned} \tag{A.20}$$

The integral on the rhs of equation (A.20) can be evaluated for $b\hat{l}_p m\kappa^2 \gg 1$ which is true for $l_{cut} \gg b\kappa$. In this approximation

$$\frac{2l_B\alpha^2}{\pi}\sum_{m=l_{cut}}^{N}(N-m)\left(\frac{2b\hat{l}_p m}{3}\right)^2\frac{3\sqrt{\pi}}{8\kappa^2}\left(\frac{3}{b\hat{l}_p m}\right)^{5/2}$$
$$\approx \frac{l_B\alpha^2}{\kappa^2\sqrt{b\hat{l}_p}}\sqrt{\frac{27}{\pi}}\sum_{m=l_{cut}}^{N}\frac{N-m}{\sqrt{m}} \approx 4\sqrt{\frac{3}{\pi}}\frac{l_B\alpha^2}{\kappa^2\sqrt{b\hat{l}_p}}$$
$$\times N^{3/2}\left(1-\frac{3}{2}\sqrt{\frac{l_{cut}}{N}}+\frac{1}{2}\left(\frac{l_{cut}}{N}\right)^{3/2}\right). \quad (A.21)$$

Substituting this expression into equation (A.20) and neglecting l_{cut}/N terms we finally obtain

$$\langle R^2\rangle \approx 2b\hat{l}_p N + 4\sqrt{\frac{3}{\pi}}\frac{l_B\alpha^2}{\kappa^2\sqrt{\hat{l}_p b}}N^{3/2} \approx R_0^2 + \frac{6^{1/2}}{\pi^{3/2}}\frac{B_{el}N^2}{R_0} \quad (A.22)$$

where $R_0^2 = 2b\hat{l}_p N$ and $B_{el} = 4\pi l_B\alpha^2\kappa^{-2}$.

Appendix B

We begin the discussion in this appendix by presenting calculations of the electrostatic interaction between two charged rods separated by a distance d and oriented with respect to each other with an angle γ. Let us define the unit vectors $\vec{e}_1$ and $\vec{e}_2$ which determine orientations of the rods. The distance between monomer t and s along these rods is equal to

$$\vec{r}_{s_1 s_2} = \vec{d} + b\vec{e}_1 t - b\vec{e}_2 s. \quad (B.1)$$

The total energy of electrostatic interactions between two rods in a given configuration is equal to

$$\frac{U_{el}(d,\gamma)}{k_B T} = \sum_{t,s=-\infty}^{\infty}\frac{l_B\alpha^2}{r_{ts}}\exp(-\kappa r_{ts}). \quad (B.2)$$

In performing the summation in equation (B.2) it useful to implement an integral representation for the Yukawa potential:

$$\frac{1}{r}\exp(-r\kappa) = \frac{2}{\sqrt{\pi}}\int_0^\infty \mathrm{d}x\ \exp\left(-x^2r^2 - \frac{\kappa^2}{4x^2}\right). \quad (B.3)$$

Using this integral representation we can rewrite equation (B.2) as follows:

$$\frac{U_{el}(d,\gamma)}{k_B T} = \frac{2u\alpha^2}{\sqrt{\pi}}\sum_{t,s}\int_0^\infty \mathrm{d}x\ \exp\left(-x^2 r_{ts}^2 - \frac{\kappa^2}{4x^2}\right)$$
$$= \frac{2u\alpha^2}{\sqrt{\pi}}\sum_{t,s}\int_0^\infty \mathrm{d}x\ \exp\Big(-x^2(d^2$$
$$+ b^2(t^2+s^2-2ts\cos\gamma)) - \frac{\kappa^2}{4x^2}\Big). \quad (B.4)$$

Substituting the summation over t and s by integration and performing these integrations first one has

$$\frac{U_{el}(d,\gamma)}{k_B T} = \frac{2u\alpha^2\sqrt{\pi}}{|\sin\gamma|}\int_0^\infty \frac{\mathrm{d}x}{x^2}\exp\left(-x^2d^2 - \frac{\kappa^2}{4x^2}\right)$$
$$= \frac{2\pi u\alpha^2}{|\sin\gamma|\kappa b}\exp(-\kappa d). \quad (B.5)$$

Let us now show how this interaction energy will change if two rods are bent into a circular conformation with a radius of curvature $R = b/\theta$ (see figure 1). It is useful to introduce the following system of coordinates. We will assume that the vector $\vec{d}$ coincides with the y axis and is pointing along the positive y direction. The first rod is located in the xy plane and the normal vector to the plane of the second rod makes an angle γ with the z axis. The distance r_{ts} between monomers t and s is equal to

$$r_{ts}^2 = x_{ts}^2 + y_{ts}^2 + z_{ts}^2 \quad (B.6)$$

$$x_{ts}^2 = R^2(\sin(t\theta) - \cos\gamma\sin(s\theta))^2 \quad (B.7)$$

$$y_{ts}^2 = (d + 2R - R(\cos(t\theta)+\cos(s\theta)))^2 \quad (B.8)$$

$$z_{ts}^2 = R^2(\sin\gamma\sin(s\theta))^2. \quad (B.9)$$

In writing equations (B.6)–(B.9) we have assumed that indexes s and t run between $-\infty$ and ∞ with zero located at the point of the closest approach on the y axis. For the small values of the angle θ we can simplify these equations as follows:

$$r_{ts}^2 \approx (b^2 + bd\theta)(t^2+s^2) - 2b^2 st\cos\gamma + d^2. \quad (B.10)$$

Substituting expression (B.10) into equation (B.4) and performing integrations one obtains

$$\frac{U_{el}(d,\gamma,\theta)}{k_B T} \approx \frac{2\pi l_B\alpha^2\exp(-d\kappa)}{\kappa b\sqrt{b^2\sin^2\gamma + d\theta(2b+d\theta)}}. \quad (B.11)$$

To complete this appendix we give the final answer for the electrostatic second virial coefficient with effective interaction given by equation (B.5) [52]:

$$B_{el} \approx 2b^2\int_0^{\pi/2}\sin^2\gamma\,\mathrm{d}\gamma\int_b^\infty\left(1-\exp\left(-\frac{U_{el}(r,\gamma)}{k_B T}\right)\right)\mathrm{d}r$$
$$= 2b^2\kappa^{-1}\int_0^{\pi/2}\sin^2\gamma\,(E_1(\xi/\sin\gamma)$$
$$+ \ln(\xi/\sin\gamma) + C)\,\mathrm{d}\gamma \quad (B.12)$$

where $C = 0.521$ is the Euler constant and $\xi = \frac{2\pi l_B\alpha^2}{\kappa b^2}\exp(-\kappa d_0)$ (d_0 is a hard-core diameter of a rod).

Appendix C

The Edwards–Singh variational principle [49] optimizes the difference between

$$0 = \langle\vec{R}_N^2(\{\vec{a}_k\})(H_0(\{\vec{a}_k\}) + U_{elec}^{rem}(\{\vec{a}_k\}) - H_{tr}(\{\vec{a}_k\}))\rangle_{tr}$$
$$- \langle\vec{R}_N^2(\{\vec{a}_k\})\rangle_{tr}\langle(H_0(\{\vec{a}_k\}) + U_{elec}^{rem}(\{\vec{a}_k\}) - H_{tr}(\{\vec{a}_k\}))\rangle_{tr} \quad (C.1)$$

where

$$\frac{H_0(\{\vec{a}_k\})}{k_B T} \approx N\sum_{k=1}^{N-1}\left(K_{eff}\left(\frac{k\pi}{N}\right)^2 + \hat{\mu}\right)\vec{a}_k^2 + \frac{N\hat{\mu}}{2}\vec{a}_0^2 \quad (C.2)$$

and the trial Hamiltonian, $H_{tr}(\{\vec{a}_k\})$, has the same form as the original one but with different values of the parameters K_{tr} and μ_{tr}.

Most of the averages needed for equation (C.1) have already been calculated in appendix A. The remaining ones are associated with the averages in the following form:

$$I_2 = \langle \vec{R}_N^2(\{\vec{a}_k\}) H_0(\{\vec{a}_k\})\rangle_{\rm tr} - \langle \vec{R}_N^2(\{\vec{a}_k\})\rangle_{\rm tr}\langle H_0(\{\vec{a}_k\})\rangle_{\rm tr}. \quad \text{(C.3)}$$

These averages can be obtained from the derivatives of $\langle \vec{R}_N^2(\{\vec{a}_k\})\rangle_{\rm tr}$ with respect to parameters $K_{\rm tr}$ and $\mu_{\rm tr}$:

$$\begin{aligned}
&\left\langle \vec{R}_N^2(\{\vec{a}_k\})\frac{H_0(\{\vec{a}_k\})}{k_{\rm B}T}\right\rangle_{\rm tr} - \langle \vec{R}_N^2(\{\vec{a}_k\})\rangle_{\rm tr}\left\langle \frac{H_0(\{\vec{a}_k\})}{k_{\rm B}T}\right\rangle_{\rm tr} \\
&= -K_{\rm eff}\frac{\partial\langle \vec{R}_N^2(\{\vec{a}_k\})\rangle_{\rm tr}}{\partial K_{\rm tr}} - \hat{\mu}\frac{\partial\langle \vec{R}_N^2(\{\vec{a}_k\})\rangle_{\rm tr}}{\partial \mu_{\rm tr}} \\
&\approx \frac{3N\hat{\mu}}{\mu_{\rm tr}^2} = 2b\frac{(l_{\rm p}^{\rm tr})^2 N}{\hat{l}_{\rm p}} \qquad \text{(C.4)}
\end{aligned}$$

$$\begin{aligned}
&\left\langle \vec{R}_N^2(\{\vec{a}_k\})\frac{H_{\rm tr}(\{\vec{a}_k\})}{k_{\rm B}T}\right\rangle_{\rm tr} - \langle \vec{R}_N^2(\{\vec{a}_k\})\rangle_{\rm tr}\left\langle \frac{H_{\rm tr}(\{\vec{a}_k\})}{k_{\rm B}T}\right\rangle_{\rm tr} \\
&= -K_{\rm tr}\frac{\partial\langle \vec{R}_N^2(\{\vec{a}_k\})\rangle_{\rm tr}}{\partial K_{\rm tr}} - \mu_{\rm tr}\frac{\partial\langle \vec{R}_N^2(\{\vec{a}_k\})\rangle_{\rm tr}}{\partial \mu_{\rm tr}} \\
&\approx \frac{3N}{\mu_{\rm tr}} = 2bl_{\rm p}^{\rm tr}N. \qquad \text{(C.5)}
\end{aligned}$$

Substituting averages into equation (C.1) one obtains the following expression for the Edwards–Singh variational principle:

$$\frac{\langle R_{\rm tr}^2\rangle}{R_0^2} - 1 - \frac{6^{1/2}}{\pi^{3/2}}\frac{B_{\rm el}N^2}{\langle R_{\rm tr}^2\rangle^{3/2}}\left(1 - \frac{3}{2}\sqrt{\frac{\hat{l}_{\rm p}}{bN}} + \frac{1}{2}\left(\frac{\hat{l}_{\rm p}}{bN}\right)^{3/2}\right) = 0 \quad \text{(C.6)}$$

where we introduced $\langle R_{\rm tr}^2\rangle = 2bl_{\rm p}^{\rm tr}N$ and $R_0^2 = 2b\hat{l}_{\rm p}N$.

References

[1] Dobrynin A V and Rubinstein M 2005 *Prog. Polym. Sci.* **30** 1049
[2] Barrat J L and Joanny J F 1996 *Adv. Chem. Phys.* **94** 1
[3] Ullner M 2003 *J. Phys. Chem.* B **107** 8097
[4] Lu Y, Weers B and Stellwagen N C 2002 *Biopolymers* **61** 261
[5] Hagerman P J 1981 *Biopolymers* **20** 1503
[6] Maret G and Weill G 1983 *Biopolymers* **22** 2727
[7] Sobel E S and Harpst J A 1991 *Biopolymers* **31** 1559
[8] Harrington R E 1978 *Biopolymers* **17** 919
[9] Cairney K L and Harrington R E 1982 *Biopolymers* **81** 923
[10] Reisner W *et al* 2007 *Phys. Rev. Lett.* **99** 058302
[11] Saleh O A *et al* 2009 *Phys. Rev. Lett.* **102** 068301
[12] Makita N, Ullner M and Yoshikawa K 2006 *Macromolecules* **39** 6200
[13] Hugel T *et al* 2001 *Macromolecules* **34** 1039
[14] Hsieh C C, Balducci A and Doyle P S 2008 *Nano Lett.* **8** 1683
[15] Baumann C G *et al* 1997 *Proc. Natl Acad. Sci.* **94** 6185
[16] Abels J A *et al* 2005 *Biophys. J.* **88** 2737
[17] Marko J F and Siggia E D 1995 *Macromolecules* **28** 8759
[18] Kuhn W, Kunzle O and Katchalsky A 1948 *Helv. Chim. Acta* **31** 1994
[19] Katchalsky A, Kunzle O and Kuhn W 1950 *J. Polym. Sci.* **5** 283
[20] Hermans J J and Overbeek J T G 1948 *Rec. Trav. Chim.* **67** 761
[21] Odijk T 1977 *J. Polym. Sci. Polym. Phys. Edn* **15** 477
[22] Skolnick J and Fixman M 1977 *Macromolecules* **10** 944
[23] Odijk T and Houwaart A C 1978 *J. Polym. Sci. Polym. Phys. Edn* **16** 627
[24] Schmidt M 1991 *Macromolecules* **24** 5361
[25] Muthukumar M 1987 *J. Chem. Phys.* **86** 7230
[26] Muthukumar M 1996 *J. Chem. Phys.* **105** 5183
[27] Barrat J L and Joanny J F 1993 *Europhys. Lett.* **25** 333
[28] Ullner M *et al* 1997 *J. Chem. Phys.* **107** 1279
[29] Ha B Y and Thirumalai D 1995 *Macromolecules* **28** 577
[30] Dobrynin A V 2005 *Macromolecules* **38** 9304
[31] Dobrynin A V 2006 *Macromolecules* **39** 9519
[32] Beer M, Schmidt M and Muthukumar M 1997 *Macromolecules* **30** 8375
[33] Liverpool T B and Stapper M 1997 *Europhys. Lett.* **40** 485
[34] Ha B Y and Thirumala D 1999 *J. Chem. Phys.* **110** 7533
[35] Golestanian R, Kardar M and Liverpool T B 1999 *Phys. Rev. Lett.* **82** 4456
[36] Ariel G and Andelman D 2003 *Phys. Rev.* E **67** 011805
[37] Kantor Y and Kardar M 1999 *Phys. Rev. Lett.* **83** 745
[38] Li H and Witten T A 1995 *Macromolecules* **28** 5921
[39] Netz R R and Orland H 1999 *Eur. Phys. J.* B **8** 81
[40] Manghi M and Netz R R 2004 *Eur. Phys. J.* E **14** 67
[41] Nguyen T T, Rouzina I and Shklovskii B I 1999 *Phys. Rev.* E **60** 7032
[42] Tkachenko A V 2006 *Phys. Rev.* E **74**
[43] Zandi R, Rudnick J and Golestanian R 2002 *Eur. Phys. J.* E **9** 41
[44] Micka U and Kremer K 1996 *J. Phys.: Condens. Matter* **8** 9463
[45] Micka U and Kremer K 1997 *Europhys. Lett.* **38** 279
[46] Nguyen T T and Shklovskii B I 2002 *Phys. Rev.* E **66**
[47] Everaers R, Milchev A and Yamakov V 2002 *Eur. Phys. J.* E **8** 3
[48] Ullner M and Woodward C E 2002 *Macromolecules* **35** 1437
[49] Doi M and Edwards S F 1986 *The Theory of Polymer Dynamics* (New York: Oxford University Press)
[50] Khokhlov A R and Khachaturian K A 1982 *Polymer* **23** 1742
[51] Ghosh K, Carri G A and Muthukumar M 2001 *J. Chem. Phys.* **115** 4367
[52] Fixman M and Skolnick J 1978 *Macromolecules* **11** 863
[53] Gubarev A, Carrillo J-M Y and Dobrynin A V 2009 *Macromolecules* **42** 5851–60